Prayogik Rasayan

In-vitro anticancer and catalytic activity of *Paederia foetida* conjugated gold nanoparticles (PF-AuNPs)

Chhabi Garai,[1] Sk Nurul Hasan,[1] Abir Chandan Barai,[1] Aditi Dey,[2] Subhankar Manna,[2]

Somenath Roy,[2*] Braja Gopal Bag[1*]

[1] *Department of Chemistry and Chemical Technology, Vidyasagar University, Midnapore, West Bengal 721102, India, Email: brajagb@gmail.com*

[2] *Department of Human Physiology with Community Health, Vidyasagar University, Midnapore, West Bengal 721102, India, Email: roysomenath1954@yahoo.in*

Received: January 22, 2019 | Accepted: January 29, 2019 | Published online: January 30, 2019

ABSTRACT

Among the less-studied plants, Paederia foetida (commonly known as Gandal) has been used by various ethnic tribes as food and medicine. The phytochemicals present in the leaf extract of Paederia foetida were utilized for the green synthesis of Paederia foetida conjugated gold nanoparticles (PF-AuNPs). Characterization of PF-AuNPs was carried out by SPR absorption band, HRTEM, DLS and X-ray diffraction studies. Anticancer activity of the stabilized PF-AuNPs studied against MCF-7 breast cancer cell line and HeLa cell lines revealed that the stabilized PF-AuNPs were highly effective for the apoptosis of cancer cells selectively. Catalytic activity of PF-AuNPs has also been reported.

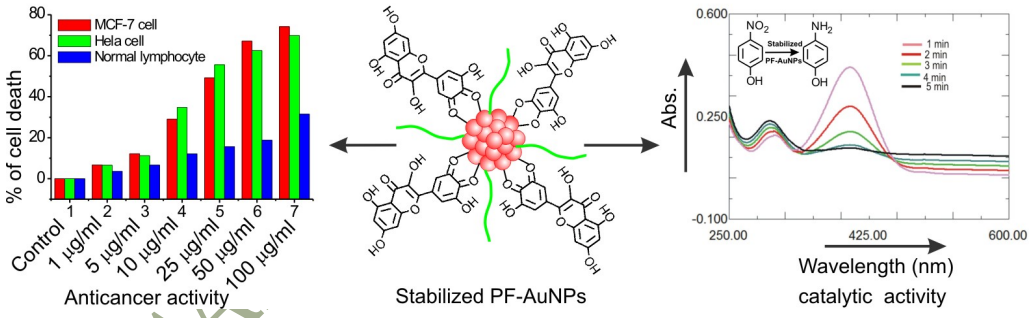

Keywords: Paederia foetida, green synthesis, gold nanoparticle, catalyst, anti-cancer, MCF-7, HeLa

1. Introduction

During last two decades metal nanoparticles have drawn increasing interest due to their distinctive features such as catalytic, optical, magnetic, electrical and medicinal activities.[1,2,3,4,5,6] Among various metal nano particles, gold nanoparticles (AuNPs) have been used as nanomedicine for diagnostic and therapeutic purposes such as carriers for the delivery of drugs [7,8] genetic materials [9] and antigens [10] and they also are used as a medicinal or diagnostic agent for the treatment of tumors [11] or rheumatoid arthritis [12] and catlyst. [13,14] A number of different physical [15] as well as chemical methods such as mechanical grinding,[16] laser irradiation,[17] electrochemical reduction,[18] photochemical reduction[19] and heat evaporation [20] have been used for the synthesis of gold nanoparticles (AuNPs). However, AuNPs synthesized under drastic conditions and stabilized with toxic chemicals limit their use in many of its applications especially in medicine and biodiagnostics. Hence, the development of an easy and efficient method for the synthesis of low-cost, energy-efficient and nontoxic gold nanoparticles is the green synthesis of AuNPs in aqueous media at room temperature utilizing the phytochemicals present in plants. [21,22] One of the advantages of using the phytochemicals present in the plant extract is that the phytochemicals can act as a reducing as well as a capping agent. Such methods have gained high significance in recent years because such a strategy will lead to "green" and "sustainable" developments.[23,24]

The green synthesis of AuNPs from the extracts of *Macrotyloma uniflorum*,[25] *Aloe-vera*,[26] *Acacia nilotica* leaf,[27] *Punica granatum*,[28] *Green coconut* shell,[29] *Abroma augusta*,[30] *Gymnema sylvestre*,[31] *Nerium oleander* [32] *etc.* have been reported in recent time. *Paederia foetida* commonly known as "Gandal" is an important ayurvedic medicinal herb, which grows mainly in tropical Asia and distributed throughout in India. It has tremendous medicinal activities and use as folk medicine in India, China, Japan and Vietnam for the treatment of inflammation, diarrhea and piles.[33] Here in we report *Paederia foetida* conjugated gold nanoparticles (PF-AuNPs) using the phytochemicals present in leaves of *Paederia foetida* at room temperature under very mild condition in aqueous medium. Additional capping or stabilizing agents were also not needed. Characterization of the stable colloidal PF-AuNPs were carried out by High Resolution Transmission Electron Microscopy (HRTEM), Energy Dispersive X-ray spectroscopy (EDX), Selected Area Electron Diffraction (SAED), SPR spectroscopy and X-Ray diffraction.

World-wide effort are ongoing from various perspective to fight against the deadly disease cancer. In recent years, phytochemical conjugated green synthesized AuNPs have shown promising results to selectively kill the cancerous cell without much adverse effects on the normal cell.[34] The *in-vitro* MTT assay carrid out by us showed a potent, selective and dose dependent anti cancer activity of the freshly synthesized PF-AuNPs on MCF-7 and HeLa cancer cell lines. Reactive Oxygen Species (ROS) measurement shows the involvement of apoptosis in cell death. Moreover, the catalytic activity of the freshly synthesized PF-AuNPs was also demonstrated for the sodium borohydride reduction of both 4-nitrophenol to 4-aminophenol and 3-nitrophenol to 3-aminophenol in aqueous medium at room temperature.

2. Experimental

2.1 Materials

The leaves of *Paederia foetida* was collected from Midnapore, West Bengal and dried in air. The details of the materials used are as reported previously.[32]

2.2 Preparation of Au (III) Solution

Preparation procedure of Au(III) solution is discussed previously.[32]

2.3 Preparation of leaf extract of *Paederia foetida* (Gandal)

Finely powdered leaf of *Paederia foetida* (2.5 g) was suspended in ethanol (25 mL) and refluxed with magnetic stirring for 1 h cooled at room temperature and then filtered. The solvent was removed to afford a green sticky solid (0.22 g). A suspendion of the leaf extract (0.0194 g) in distilled water (10 mL) was sonicated at room temperature for 10 min to yield a semi transparent solution of the leaf extract (0.194% w/v).

2.4 Synthesis of gold nanoparticles

Aliquots of Au (III) solution (0.2 mL, 14.69 mM each) were added to drop wise to the leaf extract solution contained in 4 mL vials and the final volume of the mixture was made up to 4 mL. A series of stabilized PF-AuNPs were obtained having an increasing concentration of the leaf extract from 50, 100, 200, 400, 800 to 1200 mgL^{-1} with a fixed concentration of Au (III) (0.73 mM). UV-visible spectroscopies of the solutions were carried out after twenty four hours of mixing $HAuCl_4$ and *Paederia foetida* leaf extract.

2.5 Procedure of the catalytic reduction

Catalytic activity of colloidal PF-AuNPs was demonstrated using two model reactions at room temperature: (a) the $NaBH_4$ reduction of 3-nitrophenol to 3-aminophenol and (b) the $NaBH_4$ reduction of 4-nitrophenol to 4-aminophenol.

2.6 Characterization

HRTEM, X-ray diffraction, UV-visible spectroscopy, Mass spectra are given in the supporting information.[32]

2.7 Cell Culture and Maintenance

MCF-7 breast cancer cell line and HeLa cell line were obtained from Jadavpur University, Kolkata, India. The cell line was cultured in DMEM complete media with 10% FBS (fetal bovine serum). 2 mM of L-glutamine, 100 U/mL penicillin, 100 µg/mL streptomycin was required for the culture of the cell. Cultivated cells were incubated under 5% CO2 at 37 oC temperature in a CO2 incubator. Cells were grown in an exponential form until it reaches 1x106 cells/mL growth.

2.8 Selection of Subjects for Lymphocytes

Procedure of selection and separation of Lymphocytes are reported previously.[35]

2.9 Isolation of Human Lymphocytes

Blood samples were collected according to the method of Hudson and Hay and details of this procedure are reported.[35]

2.10 Intracellular Reactive Oxygen Species Generation

The experimental details have been reported by us previously.[36,32]

2.11 Lactic dehydrogenase (LDH) releases assay

The details of LDH assay have been reported by us previously.[37]

2.12 Determination of Reduced Glutathione (GSH)

The detailed procedure for determination of GSH has been discussed in previously reported manuscript.[38]

2.13 Determination of Oxidized Glutathione (GSSG)

The detailed procedure for determination of GSSG has been discussed in previously reported manuscripts.[39,36]

2.14 Nitric Oxide Release Assay

The detailed procedure of Nitric oxide release assay has been discussed in previously reported manuscript.[38]

3. Results and Discussion

Paederia foetida, commonly known as Gandal, is a climber, bad smelling belonging to the Rubiace family. The pink coloured flowers of *Paederia foetida* occur in attum season. The leaf extract of *Paederia foetida* is rich in phytochemicals such as flavonoids, steroids, terpenoids, cardiac glycosides, cardinolides, long chain esters, etc.[40] Mass spectroscopy of an ethanolic extract of the leaves of *Paederia foetida* indicated the presence of several polyphenolic compounds including flavanoids. Indication for the presence of steroids and other plant secondary metabolites were also obtained (supporting information Figure S1).

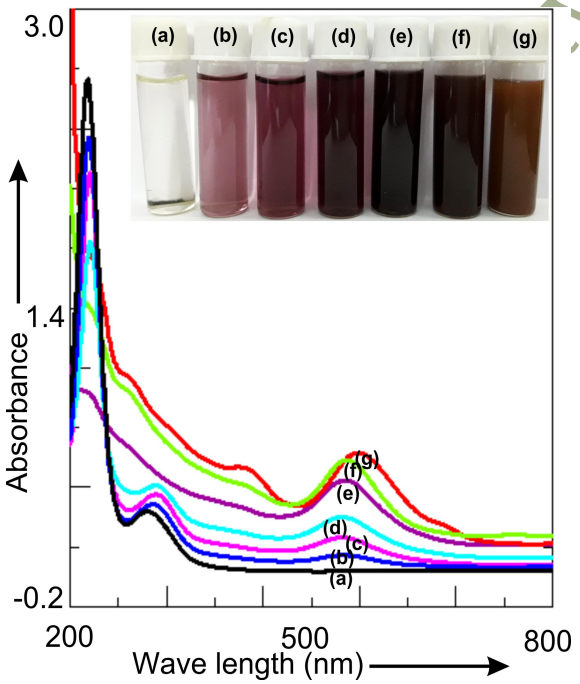

Figure 1: UV-Vis spectra of (a) $HAuCl_4$ (0.42 mM), (b-g) AuNPs at 50, 100, 200, 400, 800, 1200 mgL^{-1} concentrations of the leaf extract of *Paederia foetida*. Inset: Photograph of the PF-AuNPs.

While investigating the self-assembly of terpenoids as functional nano entities[41,42,43],and aerial oxidative coupling of 2-hydroxy-naphthalene derivatives[44] it occurred to us that the polyphenolic compounds present in the leaf extract of *Paederia foetida* and can be used to synthesize gold nanoparticles from $HAuCl_4$. When the leaves extract of *Paederia foetida* contained in a vial was treated with an aqueous solution of $HAuCl_4$ at room temperature, instant appearance of reddish color was observed visually indicating

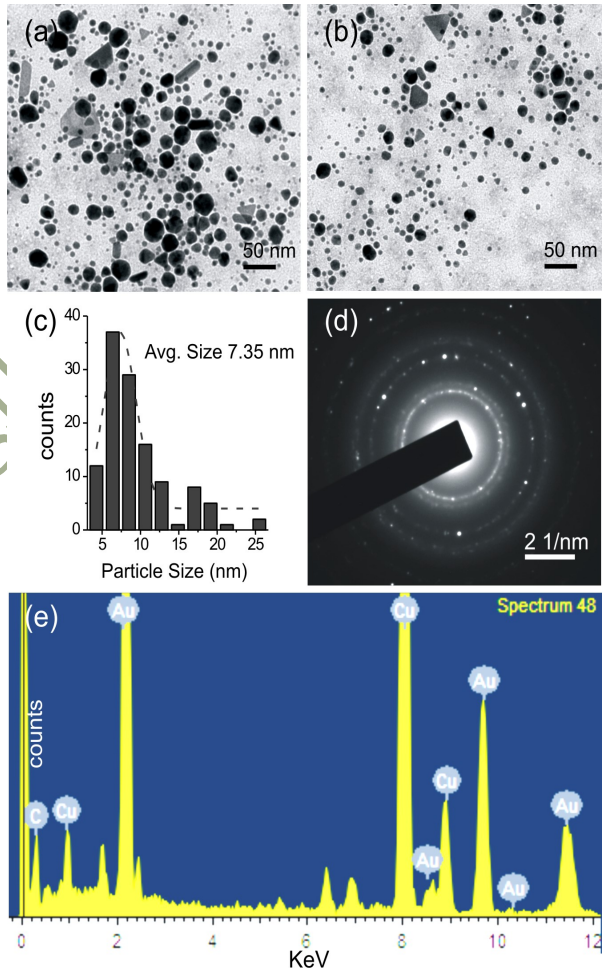

Figure 2: (a) and (b) TEM images of AuNPs , (c) Histogram of gold nanoparticles, (d) SEAD (e) EDX of stabilized PFAuNPs.

the formation of PF-AuNPs.

3.1 Characterization of synthesized PF-AuNPs

To confirm the formation of gold nanoparticles, UV-visible spectroscopy was studied. Chloroauric acid itself absorb at 290 nm for charge transfer interaction between gold ions and chloro ligands. But after addition of $HAuCl_4$ to

Paederia foetida leaf extract, the Surface Plasmon Resonance(SPR) band were formed in the region 539-559 nm (Figure1) that indicated the formation of gold nanoparticles. Increasing the concentration of the leaf extract from 50 mg L^{-1} to 100 mg L^{-1} resulted in a blue shift of the SPR band. But on further increase in the concentration of the leaf extract from 100 mg L^{-1} to 1200 mg L^{-1}, a red shif of the SPR band was observed. This observation was in consistent with the results of the DLS studies.

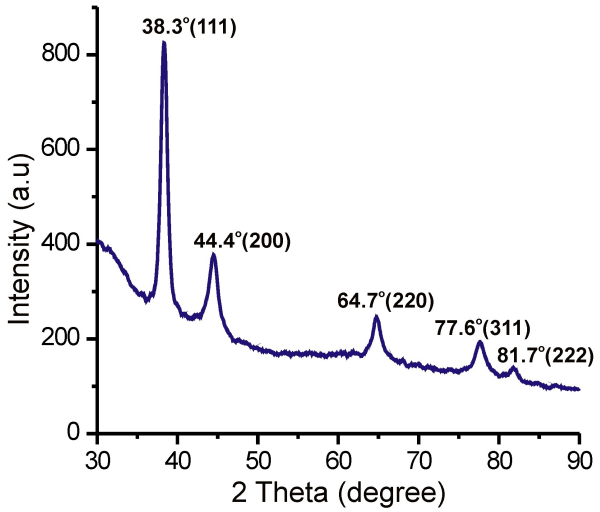

Figure 3: XRD of stabilized AuNPs synthesized from leaf extract of *Paederia foetida*.

To investigate morphologies of synthesized PF-AuNPs, HRTEM images of the sample containing 400 mg L^{-1} concentration of the leaf extract of *Paederia foetida* was recorded. HRTEM images revealed that the synthesized AuNPs were mostly spherical shaped having size range 4-25 nm along with hexagonal, triangular particles (Figure2 a,b). DLS studies carried out with PF-AuNPs synthesized using 50, 100, 200, 400 ,800,1200 mgL^{-1} of the leaf extract indicated that the size of green synthesized particles were 22 to 101 nm (supporting information Figure S2) . At 50 mg L^{-1} concentration of the leaf extract, the hydrodynamic diameters of the AuNPs were ca. 25.17 nm. With an increase in the concentration of the leaf extract to 100 mg L^{-1}, the hydrodynamic diameters of PF-AuNPs decreased to 22.36 nm due to the better stabilization of the small-sized PF-AuNPs by the leaf extract (see supporting information Figure S2). On further increase in the concentration of the leaf extract (200 and 400 mgL^{-1}), the hydrodynamic diameter of the PF-AuNPs increased further (23.64 nm and 53.19 nm). This may be due to the presence of more number of phytochemicals on the surface of PF-AuNPs at high concentration of the leaf extract.

One of the limitations dynamic light scattering (DLS) measurement is that, the instrument cannot measure the bare AuNPs. However, it is possible in the case of HRTEM studies. HRTEM study showed that the average diameter of gold nanoparticles using leaf extract 400 mg L^{-1} is 7.35 nm (Figure 2c) which is much lower than DLS measured particle size. The gold nanoparticles synthesized using leaf extract of *Paederia foetida* were very stable at room temperature because there was no aggregation of the colloidal PF-AuNPs after several months. It also confirmed by the very high negative zeta potential value of -26.6 mV to -8.99 mV (supporting information Figure S3).

X-ray diffraction analysis was carried out with the stabilized PF- AuNPs coated over a glass plate (Figure 3). The reflections of the planes (111), (200), (220), (311) and (222) observed at 2θ = 38.3°, 44.4°, 64.7°, 77.6° and 81.7° respectively supported reduction of Au(III) to Au(0) by the phytochemicals present in the leaf extract of *Paederia foetida* and also confirms the crystallinity of gold atoms. The predominant orientation of the (111) plane is manifested by the highest intensity of the (111) plane compared to others peaks. EDX analysis of synthesized PF-AuNPs was further evidence for the formation of gold nanoparticles (Figure 2e).

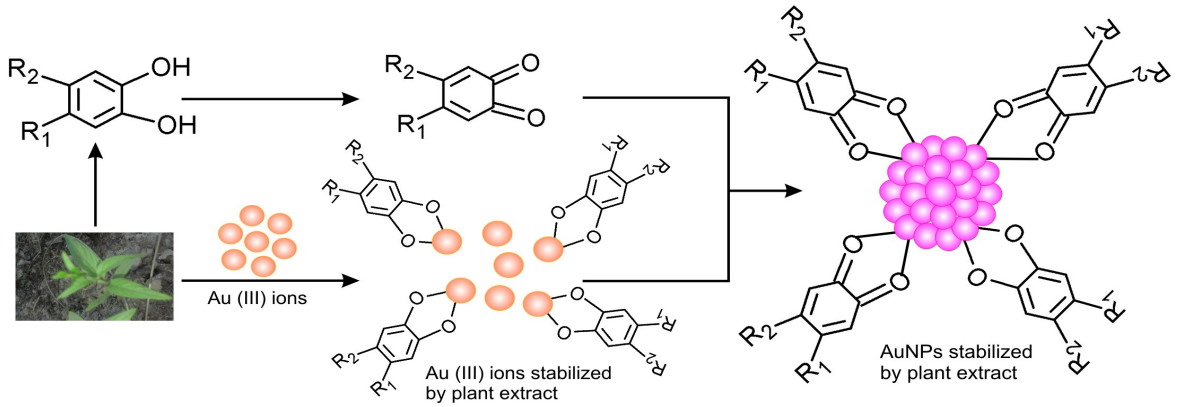

Figure 4: Mechanism of the formation AuNPs and its concomitant stabilization by the phytochemicals present in leaf extract of *Paederia foetida*.

3.2 Mechanism of the formation and stabilization of PF-AuNPs

Mass spectral analysis of the leaf extract indicated the presence of several polyphenolic compounds such as Chrysin (M+ 255), Quercetin (M+ 302), Quercetrin (M+ 446) etc. (Figure S1). Taking a o-dihydroxyphenolic compound as a representative, a schematic representation of a plausible mechanism for the synthesis and stabilization of PF-AuNPs is shown in Figure 4. The details of the mechanistic explanation for the formation of PF-AuNPs have been reported by us previously [28,29,30,32] and it is also given in the supporting information.

4. Application of Stabilized PF-AuNPs

To demonstrate the usefulness of the stabilized PF-AuNPs, biological activity along with in-vitro anticancer activity and catalytic activity were studied which are discussed in the following sections.

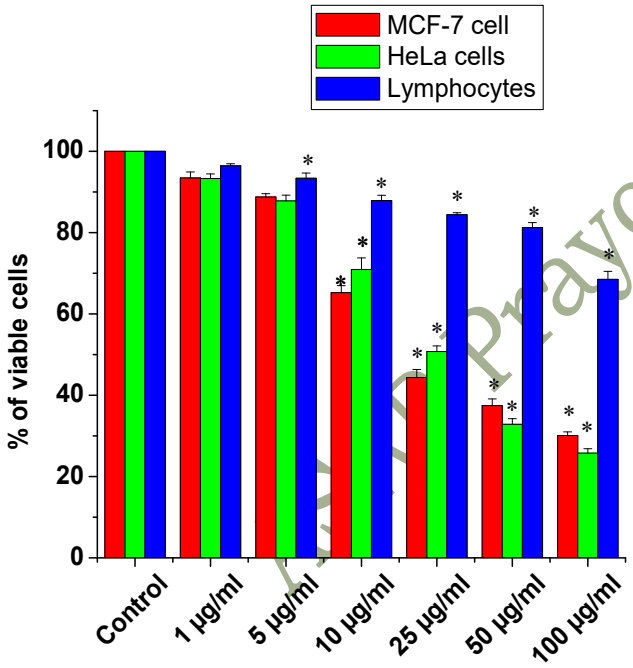

Figure 5: In vitro cell viability assay of drug (synthesized AuNPs) treated on normal PBL, HeLa cell and MCF-7 Cell-lines were treated with the drug for 24 hours at 37 °C. Cell viability was measured by the MTT method and the details are given in the supporting information. Values are expressed as mean ± SEM of experiments; superscripts indicate significant differences ($p < 0.05$) compared with the control group.

4.1 Biological activity and application as an anti-cancer drug of stabilized PF-AuNPs

To find out whether PF-AuNPs can act as a drug, dose dependent cytotoxicity assay of the freshly prepared PF-AuNPs (0.5 mL, 400 mgL^{-1}, synthesised with $HAuCl_4$ (0.73 mM) was carried out on MCF-7 cell line and HeLa cell lines. Non-radioactive colorimetric assay technique using tetrazolium salt, 3-[4,5-dimethylthiazole-2-yl]-2,5-diphenyl tetrazolium bromide (MTT) was used for the cell viability studies.

The % of cell viablility was calculated by using the following equation. [36]

$$\% \text{ of cell viability} = [OD_{sample} - OD_{control}] \times 100/OD_{control}$$

With drug concentration of 1 µg/mL, 5 µg/mL, 10 µg/mL, 25 µg/mL, 50 µg/mL and 100 µg/mL , the % of MCF-7 breast cancer cells and HeLa cells killed were 6.54, 11.22, 34.78, 55.64, 62.55 , 69.91 and 6.69, 12.19 , 29.07 , 49.24 , 67.15, 74.23 respectively.

The half inhibitory concentration (IC_{50}) value showed by the drug that the concentration required to inhibit the 50% of MCF-7 cells and HeLa cells growth were 47.45 and 48.43µg/mL respectively (supporting information Figure S4 & S5). Multiple linear regressions were used for comparison of data through statistica version 5.0 (Stat soft, India) software pakage.

From the graph which is obtained from MTT assay, we calculated the % of cell death in case of both the cancer cell lines as well as in normal lymphocytes after the treatment of the drug (PF-AuNPs). The drug showed potent anti-cancer activity towards both cancer cells. The killing ability of the drug (PF-AuNPs) against cancer cell lines were significantly higher compared to control group .The dose dependent cytotoxicity assay was also done using normal lymphocyte. 50 µg/mL dose of the drug can be used as a biologically safe dose because at this particular dose it killed the cancer cell massively and the cytotoxicity is minimum (Figure 5). We observed that IC_{50} value of both the cancer cell (MCF-7 and HeLa cell) were 47.45 and 48.43µg/mL respectively after the treatment with PF-AuNPs. So, we have choosen 50µg/mL dose for both the cell for further biological experiment throughout the study.

4.1.1 Intracellular Reactive Oxygen Species (ROS) measurement

ROS are short-lived and active molecules containing oxygen which are essential for normal physiological activity but the overproduction of ROS are responsible for cell death.[45] ROS are generated from different metabolic process, mainly mitrochondrial respiratory chain[46] and neutralize by various anti-oxidant enzyme. Metal nanoparticles are able to produce higher amount of ROS inside the cancer cell.[47] Excessive production of ROS indicates dysfunction of mitochondria, higher level of metabolic activity and oncogene activity. High level of ROS generation in cancer cell showed apoptosis through arresting the cancer cell cycle.[48] In the present study, we have treated the MCF-7 cells and HeLa cells with the synthesized PF-AuNPs at 50 µg/mL dose for 24

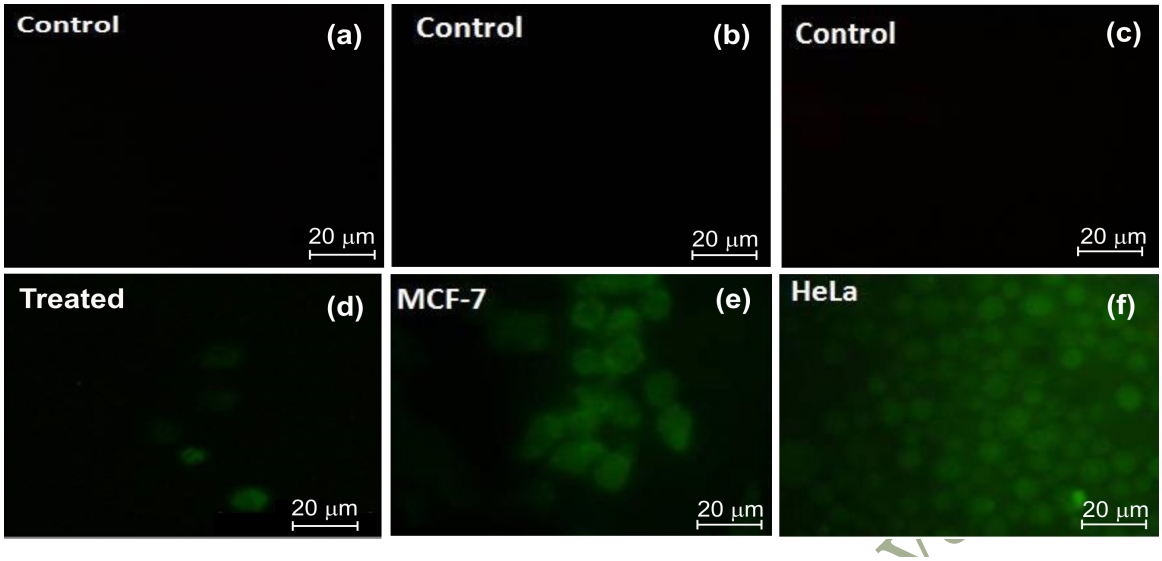

Figure 6: ROS production by the drug (synthesized AuNPs) .(a),(b),(c) are the control of normal lymphocyte,MCF-7 cell line and HeLa cell line. (d),(e),(f) are the drug treated normal lymphocyte,MCF-7 cell line. .and HeLa cell line.

hr. After the schudeled experimental time, we observed significant amount of ROS generation inside the both cancer cells. The microscopic images are evidence of for production of ROS (Figure 6). At the same time normal cells were remain almost unaffected and the PF-AuNPs can be used as a drug for further cancer treatment.

4.1.2 LDH release level

LDH is cytoplasmic enzyme presents in all living cells which converts lactate to pyruvate and back . When the released amount of LDH was increased compared to control group in the extracellular space that incident indicates the damage of cell membrane.[49] In the present study the LDH release was significantly increased by 37.39% after the treatment with PF-AuNPs as compared to control in MCF-7 cancer cell and by 45.92% in HeLa cell lines at 50 μg ml^{-1} dose. (supporting information Figure S6)

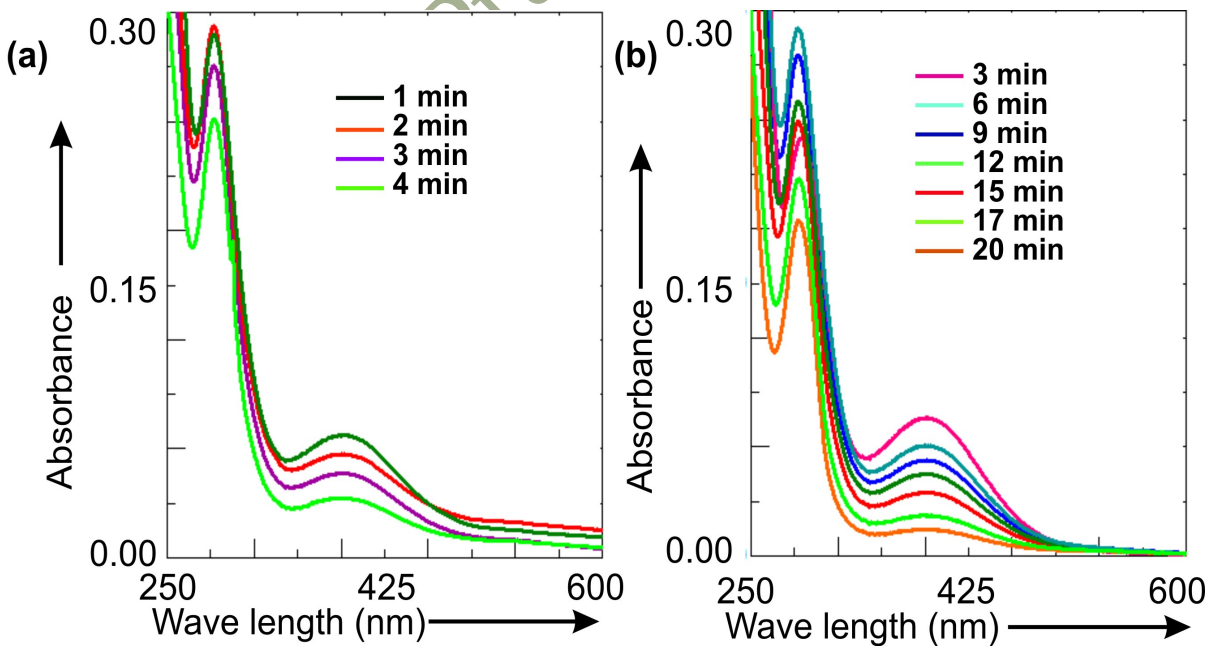

Figure 7 : UV-Visible spectra at different time interval during the catalytic reduction of 3-nitro phenol to 3-amino phenol using (a) 0.05 mL & (b) 0.025 mL of stabilized diluted PF-AuNPs

4.1.3 Cellular redox status (GSH and GSSG levels)

At normal physiological condition Glutathione present in reduced from but after the treatment with nanoparticles, overproduction of ROS oxidized the Glutathione enzyme. So, the level of GSSG was increased in cancer cells.[50] Our present study showed that PF-AuNPs decrease the levels of GSH in cancer cells . PF-AuNPs was able to decrease the GSH level significantly ($P<0.05$) in the MCF-7 cell line by 48.65%, and in the Hela cell lines by 55.62% at 50 μg ml^{-1} dose (supporting information Figure S7 a). The level of GSSG was elevated after the treatment of gold nanoparticles in both the MCF-7 cell and HeLa cell. After PF-AuNPs treatment, GSSG levels in the MCF-7 cell line and HeLa cell line were increased significantly ($P<0.05$) by 49.24% and 72.17% respectively at the dose of 50 μg ml^{-1} (supporting information Figure S7 b).

4.1.4 Nitric oxide release level

Nitric oxide release was elevated in PF-AuNPs-treated cells. The NO level in the MCF-7 and Hela cell line were significantly ($P<0.05$) increased by 68.93% and 106.94% respectively at 50 μg ml^{-1} dose (supporting information Figure S8).

4.2 Catalytic Activity

Though, metallic gold is usually inactive as a catalyst, excellent catalytic activities have recently been demonstrated for various chemical transformations. This is mostly due to its very high surface to volume ratio compared to the bulk metal. We investigated the utilization of PF-AuNPs as a catalyst for the degradation of toxic pollutants 3- and 4-nitrophenols by reduction in presence of sodium borohydride.

4.2.1 Reduction of 3-nitrophenol to 3-aminophenol by the stabilized PF-AuNPs

Reduction of nitro-phenol to amino phenol using $NaBH_4$ is thermodynamically favoured reaction. But after addition of aqueous sodium borohydride (16.39 mM) to a solution of 3-nitro phenol (0.05mM), the absorption band was shifted to 392 nm from 331 nm due to the formation of 3-nitro phenolate. But 3-amino phenolate was not formed. Then, an aliquot of 3-NP was treated with freshly prepared aqueous $NaBH_4$ solution in the presence of stabilized colloidal PF-AuNPs (0.1 mL, synthesized with 50 mg L^{-1} leaf extract). The 3-nitrophenolate ion peak at 392 nm completely disappeared within 30 s and a new peak around 300 nm was concomitantly formed demonstrating the excellent catalytic activity of PF-AuNPs. But due to very fast reaction, kinetics of the reaction could not be studied. For calculating the catalytic rate constant by slowing down the rate of reaction, the concentration of the catalyst was reduced to 1/10th (0.1 mL of colloidal PF-AuNPs of 50 mg/L was diluted to 1 mL with distilled water). In this case, after the addition of 0.05 ml diluted PF-AuNPs, the reaction was complete within 4 min with disappearance of the 3-nitrophenolate ion peak. Similarly on addition of 0.025 mL of diluted PF-AuNPs to the reaction mixture, the intensity of the peak at 331 nm reduced slowly and disappeared completely in 20 minutes (Figure 7).

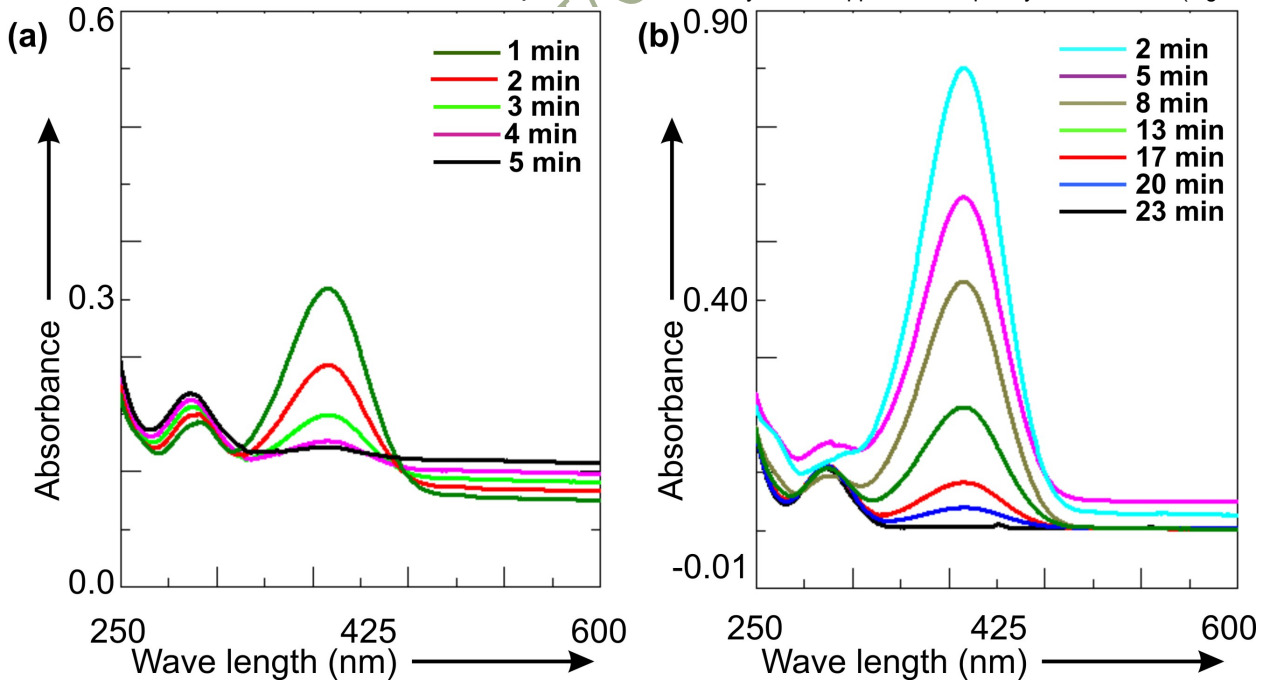

Figure 8: UV–Visible spectra at different time interval during the catalytic reduction of 4-nitro phenol to 4-amino phenol using (a) 0.1 mL & (b) 0.05 mL of stabilized diluted PF-AuNPs.

For these reduction reactions, the rate constants were calculated as 3.37 x 10^{-3} sec^{-1} and 1.31x10^{-3} sec^{-1} respectively (supporting information Figure S9) that is comparable with the values obtained by us and others reported previously.[31,32]

4.2.2 Reduction of 4-nitrophenol to 4-aminophenol by the stabilized PF-AuNPs

During $NaBH_4$ (16.39 mM) reduction of 4-nitro-phenol (0.05 mM) the absorption band at 318.5 nm shifted to 401 nm due to the formation of 4-nitrophebnolate anion by addition of $NaBH_4$. But reduction of nitro to amino did not take place even after several days. Interestingly, on addition of 0.1 mL of diluted stabilized PF-AuNPs (synthesized with 50 mgL^{-1} concentration of the leaf extract) to the reaction mixture, the intensity of the peak at 401 nm for the 4-nitrophenolate ion completely disappeared in 7 min with comcomitant appearance of a new peak around 318 nm indicating the formation of 4-aminophenolate. The rate constant value from UV-vis data was calculated to be 5.6 x 10^{-3} sec^{-1} (supporting information Figure S9 c). Similarly on addition of 0.05 mL of diluted stabilized PF-AuNPs to the reaction mixture, the peak for 4-nitrophenolate ion slowly decreased and completely disappeared in 23 minutes with concomitant appearance of a new peak for 4-aminophenolate ion (Figure 8). The rate constant value for this reduction was calculated to be 2.74 x 10^{-3} sec^{-1} (supporting information Figure S9 d) that is comparable to the values reported by us and others previously.[14,30]

5. Conclusion

Evidence for the presence of polyphenols has been obtained in the leaf of *Paederia foetida*. The phytochemicals present in the leaf extract have been utilized for the synthesis of gold nanoparticles at room temperature under very mild conditions without any additional stabilizing agents. According to our knowledge, this is the first report of green synthesis of gold nanoparticles utilizing leaf extract of *Paederia foetida*. A schematic representation for the formation of stable PF-AuNPs has also been demonstrated. The present study also showed the *in-vitro* anti cancer activity of the stabilized PF-AuNPs on MCF-7 cell lines and HeLa cell lines indicated that significant killing of the cancer and HeLa cell lines at 47.45 and 48.43 µg/mL respectively. The normal lymphocytes remained almost unaffected at this dose. The catalytic activities of the stabilized PF-AuNPs have also been demonstrated for the reduction of 3- and 4-nitrophenols to their corresponding aminophenols.

6. Acknowledgements

CG, SNH and ACB thank UGC, New Delhi and AD thank DST-Inspire for fellowships. BGB thanks **India-Srilanka** project (DST/INT/SL/P25/2016), SERB, India (EMR/2016/001123), UGC-SAP DRS II, DST-FIST New Delhi and Vidyasagar University for financial support and infrastructural facilities funding.

7. References

1. A.M. Alkilany, S.E. Lohse, C.J. Murphy, *Acc. Chem. Res.* **2013,** 46, 650.
2. Y. Zhang, X. Cui, F. Shi, Y. Deng, *Chem. Rev*. **2012,** 112, 2467.
3. C.J. Murphy, A.M. Gole, J.W. Stone, P.N. Sisco, A.M. Alkilany, E.C. Goldsmith, S.C Baxter, *Acc. Chem. Res.* **2008,** 41, 1721.
4. K.G. Thomas, P.V Kamat, *Acc. Chem. Res*. **2003,** 36, 888.
5. N.L. Rosi, C.A. Mirkin. Nanostructures in Biodiagnostics. *Chem. Rev*. **2005,** 105, 1547–1562.
6. M.M.R. Mollick, B. Bhowmick, D. Maity, D. Mondal, M.K. Bain, K. Bankura, S. Joy, D. Rana, K. Acharya, D. Chattopadhyay, *International Journal of Green Nanotechnology* **2012,** 4, 230.
7. G.F. Paciotti, L. Myer, D. Weinreich, D. Goia, N. Pavel, R.E. McLaughlin, L. Tamarkin, *Drug Delivery* **2004,** 11, 169.
8. P. Ghosh, G. Han, M. De, C.K. Kim, V.M Rotello, *Adv. Drug Delivery Rev*. **2008,** 60, 1307.
9. J.J. Donnelly, B. Wahren, M.A. Liu, *J. Immunol.* **2005,** 175, 633.
10. L.A. Dykman, V.A. Bogatyrev, *Russ. Chem. Rev*. **2007,** 76, 181.
11. E. Boisselier, D. Astruc, *Chem. Soc. Rev*. **2009**, 38, 1759.
12. C.L. Brown, M.W. Whitehouse, E.R.T. Tiekink, G.R. Bushell, *Inflammopharmacology* **2008,** 16, 133.
13. C.D. Pina, E.Falletta, M. Rossi, . *Chem. Soc. Rev.* **2012,** 41, 350.
14. A. Corma, H. Garcia, *Chem. Soc. Rev*. **2008**, 37, 2096.
15. Y. Ishida, R.D. Corpuz, T. Yonezawa, *Acc. Chem. Res.* **2017,** 50, 2986.
16. V. Šepelák , S.B. Colin, G.L. Caër, *Dalton Trans.* **2012,** 41, 11927.
17. H. Wang, M. Lau, T. Sannomiya, B. Gökce, S. Barcikowski, O. Odawara, H. Wada, *RSC. Adv.* **2017,** 7, 9002.
18. Y. Gao, J. Hao, *J. Phys. Chem. B.* **2009,**113, 9461.
19. S. Eustis, H.Y. Hsu, M.A.E. Sayed, *J. Phys. Chem. B.* **2005,**109, 4811
20. C.H. Chon, S. Paik, J.B. Tipton, K.D. Kihm, *Langmuir* **2007,** 23, 2953.
21. J.A. Dahl, B.L.S. Maddux, J.E. Hutchison,. *Rev.* **2007,** 107, 2228.
22. J.M. Campelo, D. Luna, R. Luque, J.M. Marinas, A.A. Romero, *Chem.Sus.Chem*. **2009,** 2, 18.
23. S. Iravani, . *Green Chem*. **2011,** 13, 2638.

24. P. Elia, R.S. Zach, S.Hazan, Z.P. Kolusheva, Y. Zeiri, *Int. J. Nanomedicine* **2014,** 9, 4007.
25. S.A. Aromal, V.K. Vidhu, D. Philip, *Spectrochim Acta A Mol Biomol Spectrosc* 2012, 85, 99.
26. S.P. Chandran, M. Chaudhary, R. Pasricha, A. Ahmad, M. Sastry , *Biotechnol Prog*. **2006,** 22, 577.
27. R. Majumdar, B.G. Bag, N. Maity. *Int. Nano Lett*. **2013,** 3, 2-6.
28. S.S. Dash, B.G. Bag, *Appl. Nanosci*. **2014,** 4, 55.
29. K. Paul, B.G. Bag, K. Samanta, *Appl. Nanosci.* **2014,** 4, 769.
30. S. Das, B.G. Bag, R. Basu, *Appl. Nanosci*. **2015,** 5, 867.
31. S.N. Hasan, K. Paul, A. Dey, S. Manna, S. Roy, B.G. Bag, C. Mukhopadhyay, *Int. J. Res. Chem. Environ*. **2017**, 7, 1.
32. A.C. Barai, K. Paul, A. Dey, S. Manna, S. Roy, B.G. Bag, C. Mukhopadhyay, *Nano Convergence* **2018,** 5, 10, doi.org/10.1186/s40580-018-0142-5
33. L. Wang, Y. Jiang, T. Han, C. Zheng, L. Qin, *Nat. Prod. Commun*. **2014,** 9, 879.
34. J.G. Nirmala, S. Akila, M.S.M.M. Nadar, R.T. Narendhirakannan, S. Chatterjee, *RSC. Adv.* **2016**, 6, 82205.
35. L. Hudson, F.C. Hay. Practical Immunology 3rd ed. Blackwell Publishing: UK, 1989.
36. S.K. Dash, T. Ghosh, S. Roy, S. Chattopadhyay, D. Das, *J. Appl. Toxicol*. **2014**, 34:1130.
37. S.K. Dash, S. Chattopadhyay, T. Ghosh, S.S. Dash, S. Tripathy, B. Das, B.G. Bag, D. Das, S. Roy, *Biomedicine & Pharmacotherapy* **2015,** 72, 144.
38. S.P. Chakraborty, S.K. Mahapatra, S.K. Sahu, S. Das, S. Tripathy, S. Dash, P. Pramanik, S. Roy, *Oxid Med Cell Longev*. **2011**doi: 10.1155/2011/942123
39. S.P. Chakraborty, S. Roy, *Asian Pac J Trop Biomed.* **2014,** 4, 298.
40. (a) M. Thirupathi, D. Srinivas, K. Rajendar, D. Raju, R.K. Jaganmohan, *J Atoms Mole*. **2013,** 3, 17. (b) K.C. Wong, G.L. Tan, *J. Flavour Fragr*. **1994, 9**, 25. (c) M.U. Ahmad, M.R. Islam, E. Huo, M.W. Khan, S. Gupta, *J. Bangladesh Acad Sci***. 1991,** 15, 19.
41. B.G. Bag, R. Majumdar. Self-assembly of Renewable Nano-sized Triterpenoids. *Chem. Rec.* **2017, 17,** 841-873.
42. B.G. Bag, A.C. Barai, K. Wijesekera, P. Kittakoop, *ChemistrySelect* **2017,** 2, 4969.
43. B.G. Bag, N. Hasan, P. Pongpamorn, N. Thasana, *ChemistrySelect* **2017,** 2, 6650.
44. B.G., Bag, S. Ghorai, S.K. Panja, S.K. Dinda, K. Paul, . *RSC Adv*. **2018,** 8, 29155.
45. K. Rahman. Studies on free radicals, antioxidants and co-factors. *Clin. Interv. Aging* **2007,** 2, 219-236.
46. V. Vallyathan, X. Shi, Env. *Health Perspectives* **1997, 105**, 165.
47. A.A. Kajani, A.K. Bordbar, S.H.Z. Esfahani, A.R. Khosropourb, A. Razmjou, *RSC Adv*. **2014**, 4, 61394.
48. E. Cadenas, *Mol Aspects Med*. **2004,** 25, 17.
49. J.F. Burd, G.M.A. Usategui, . *Clin Chim Acta* **1973,** 46, 223.
50. E. Beutler, *J. Clin. Invest.* **1969,** 48, 1957.